IceSynth II: Synthesis of SAR Sea-Ice Imagery Using Region-Based Posterior Sampling

Alexander Wong, *Student Member, IEEE*, Peter Yu, Wen Zhang, *Student Member, IEEE*, and David A. Clausi, *Senior Member, IEEE*

***Abstract*—A novel method for synthesizing synthetic aperture radar (SAR) sea-ice imagery named IceSynth II is presented. A Markov random field model is assumed, and a conditional sampling approach is used to learn local conditional posterior probability distributions on a regional basis. Synthetic SAR sea-ice images and the associated ground-truth segmentations are generated using a region-based posterior sampling approach. Experimental results using single-polarization RADARSAT-1 and dual-polarization RADARSAT-2 SAR sea-ice imagery provided by the Canadian Ice Service show that IceSynth II is capable of producing SAR sea-ice imagery that is more realistic than existing approaches. The synthesized images are well suited for performing systematic and reliable objective evaluation of SAR sea-ice image segmentation methods.**

***Index Terms*—Conditional, Markov random field (MRF), multivariate region growing, posterior sampling, sea ice, synthesis, synthetic aperture radar (SAR).**

I. Introduction

AN IMPORTANT tool in the daily monitoring of conditions in ice-infested regions is spaceborne synthetic aperture radar (SAR) imagery obtained using satellites such as RADARSAT-1/2. Acquired SAR sea-ice imagery is interpreted by analysts to produce daily sea-ice charts for operational purposes such as ship navigation [1].

The laborious nature of manual SAR sea-ice segmentation has led to the development of automated approaches [2]–[6]. To evaluate the effectiveness of a SAR sea-ice segmentation algorithm for operational use, qualitative assessment by trained experts is common and pragmatic. Preferably, accurate sensor-resolution ground truth should be made available, but these are time consuming to produce particularly with respect to the volumes of data necessary for robust operational validation. Evaluating SAR sea-ice segmentation methods in a reliable and systematic fashion is thus difficult.

An intuitive approach to address these issues is to synthesize imagery for evaluating SAR sea-ice segmentation methods in a systematic manner. The research literature has focused on general SAR texture synthesis [7]–[10], which is inadequate for producing realistic SAR sea-ice images consisting of both sea-ice textures and multiscale structures. Recently, a system was developed to synthesize sea-ice imagery with both texture and multiscale sea-ice structures [11]. This method produced natural looking formations but lacked a coupled SAR sea-ice texture and structure generation process, leading to synthetic images with a disjointed appearance. The goal here is to produce imagery that appears natural and largely indistinguishable from real SAR sea-ice imagery.

This letter contributes IceSynth II, a novel algorithm for synthesizing SAR sea-ice imagery by statistical sampling of local regions. The algorithm works under the principle that the statistical, structural, and textural characteristics of a particular region is conditioned on the characteristics of the neighborhood around it. By learning the conditional probability distributions of these characteristics from real SAR sea-ice imagery, synthetic SAR sea-ice imagery can be generated with the same characteristics as the real imagery. Furthermore, the synthesis algorithm generates an associated ground truth that can be used to objectively evaluate SAR sea-ice segmentation methods.

The underlying theory is described in Section II. Synthesis results using operational single-polarization RADARSAT-1 and dual-polarization RADARSAT-2 SAR sea-ice imagery provided by the Canadian Ice Service (CIS) are presented and discussed in Section III.

II. Region-Based Posterior Sampling

Research in SAR image synthesis has been focused on model-based stochastic synthesis [7]–[10], where random fields are developed using statistical models based on radar theory such as Weibull, log normal, exponential, gamma, and K-distribution models [12]. Unfortunately, such model-based approaches require many parameters (e.g., incidence angle, physical properties of sea-ice types, SAR platform intrinsic properties, etc.) and are hence difficult to configure. More importantly, such approaches do not take sea-ice structure (such as the spatial distribution of different ice types) into account and, as such, cannot be used to generate realistic SAR sea-ice imagery. SAR data can also be generated from a known reflection map of the scene [13] but the map must still be synthesized with the structural characteristics of sea ice.

Wong *et al.* [11] address the sea-ice image synthesis problem by generating SAR sea-ice texture and multiscale structures independently based on real SAR sea-ice texture and structure priors. However, since the structure and texture models are learned independently, the resulting synthetic imagery exhibits

Manuscript received June 21, 2009; revised August 27, 2009. Date of publication November 24, 2009; date of current version April 14, 2010. This work was supported in part by the Natural Sciences and Engineering Research Council of Canada via an individual Discovery Grant and in part by the Canadian Federal Government's International Polar Year program.

The authors are with the Vision and Image Processing Research Group, Department of Systems Design Engineering, University of Waterloo, Waterloo, ON N2L 3G1, Canada (e-mail: alexanderwong@einfodaily.com; p5yu@engmail.uwaterloo.ca; wxzhang@engmail.uwaterloo.ca; dclausi@engmail.uwaterloo.ca).

Digital Object Identifier 10.1109/LGRS.2009.2035136

an undesirable disjoint appearance. An intuitive approach to addressing this issue is to learn both the SAR sea-ice texture and structures within the same statistical model. Therefore, we propose learning from real SAR sea-ice imagery on a regional basis rather than a pixel basis as both structure and texture characteristics are preserved within a region.

The proposed region-based local conditional posterior sampling approach can be described as follows. Let S be a set of sites (pixels) on a discrete lattice $\mathcal{L}$ and $s \in S$ be a site in $\mathcal{L}$. Let $X = \{X_s | s \in S\}$, $C = \{C_s | s \in S\}$, $Y = \{Y_s | s \in S\}$, and $D = \{D_s | s \in S\}$ be random fields on S, with X_s and C_s taking on values representing the *a priori* tonal and ground-truth ice types of the *real* SAR sea-ice image prior at site s, respectively. Y_s and D_s are values representing the tonal values and ground-truth ice types of the *synthesized* SAR sea-ice image at site s. Let $x = \{x_s | s \in S\}$, $c = \{c_s | s \in S\}$, $y = \{y_s | s \in S\}$, and $d = \{d_s | s \in S\}$ be realizations of X, C, Y, and D that form the real SAR sea-ice image prior, the real ground truth image, the synthesized SAR sea-ice image, and the synthesized ground truth image, respectively. Let r represent a region consisting of a set of connected sites. Furthermore, let N_r be a local neighborhood of connected sites encapsulating region r that has been populated. N_r and r do not share sites. Finally, let SAR sea-ice imagery be modeled as a Markov random field (MRF) [14], where the probability distribution of X_r given N_r is independent of the rest of X.

Based on this MRF model, the synthesized SAR sea-ice image region y_r and the associated synthesized ground truth d_r can be synthesized by performing posterior sampling according to the local conditional probability distribution $P(y_r|N_r)$. To learn $P(y_r|N_r)$, we employ a nonparametric conditional sampling approach where all region samples $\{\rho_1, \rho_2, \ldots, \rho_m\}$ from x satisfying the following condition are drawn to estimate $P(y_r|N_r)$:

$$\Upsilon(N_r, N_\rho) < (1+\tau)\Upsilon\left(N_r, N_{\rho_\gamma}\right) \tag{1}$$

where Υ is the cumulative squared distance between N_r on y and N_ρ on x

$$\Upsilon(N_r, N_\rho) = \sum \left(y_{N_\rho} - x_{N_\rho}\right)^2 \tag{2}$$

and ρ_γ is the region sample that minimizes Υ

$$\rho_\gamma = \arg\min_{\rho} \Upsilon(N_r, N_\rho) \tag{3}$$

and where τ is a positive (i.e., $\tau > 0$) rejection threshold which limits the number of regions that are drawn to those which have a certain level of similarity to N_r.

The synthesis algorithm is implemented as follows:

1) Starting with y and d as blank image arrays, fill initial region r_{iy} in y with a random region r_{ix} from x. Fill r_{iy} in d with values from r_{ix} in c.
2) Region r_{fy} is a region immediately adjacent to r_{iy} in y that is to be filled next in the raster scan, as follows:
   a) Randomly choose a neighborhood N_ρ in x from the set of all neighborhoods in x that satisfies (1) with $N_{r_{fy}}$, the neighborhood of r_{fy}.
   b) Fill r_{fy} in y and d using the values from the region r_{fx} in x and c, respectively, where r_{fx} is the region that has pixels in the same relative spatial position to N_ρ as r_{fy} has to $N_{r_{fy}}$.
3) Step 2 is repeated with an adjacent unfilled region in the raster scan until the entire synthetic image is filled.

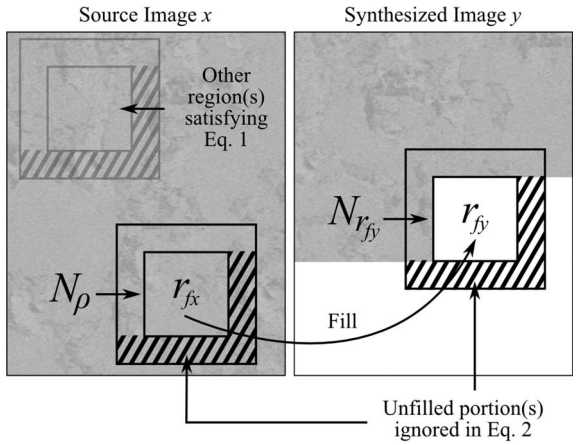

Fig. 1. Region r_{fy} is filled with region r_{fx}, selected from all candidate regions that satisfy (1).

If a pixel-level ground truth is available for the source image, the algorithm will fill in the pixels in the synthetic ground-truth image corresponding to r_{fy} with the pixels in the source ground-truth image corresponding to r_{fx}.

Fig. 1 shows the algorithm in operation, with the synthetic image having been partially filled. Portions of the neighborhood $N_{r_{fy}}$ that are unfilled in the synthetic image are ignored in the calculation of (2). Currently, the algorithm does not take the SAR incidence angle into account but a future extension might do so by only sampling from neighborhoods in the source image that have the same incidence angle as the region to be filled. To avoid incidence angle-related problems, only images that do not exhibit incidence angle-induced variations in appearance were chosen as test images.

The region and neighborhood sizes are parameters which must be set. The sizes must be large enough to capture the structural characteristics of sea-ice-like floe or lead sizes. For the experiments here, r_{fy} is a region that is 50 by 50 pixels in size and $N_{r_{fy}}$ is an 8 pixel border neighborhood around r_{fy}. Hence, the region and the border neighborhood combined is 66 by 66 pixels in size. These parameter values were found experimentally to produce reasonable results for source images with a spatial resolution of 100 m per pixel.

The rejection threshold τ is not explicitly set. Its value is allowed to float such that for every region to be filled, five neighborhoods satisfy (1). This number of neighborhoods was also determined experimentally. If more neighborhoods are allowed to satisfy (1), the synthetic image will have discontinuities as dissimilar regions will be used to fill each r_{fy}. If fewer neighborhoods are permitted, the variety of synthetic images that can be generated from one source image is limited.

The proposed region-based local conditional posterior sampling approach has two important advantages over existing approaches. First, because both SAR sea-ice structure and texture characteristics are integrated into a common statistical model, the synthetic image does not appear disjointed. Second, unlike

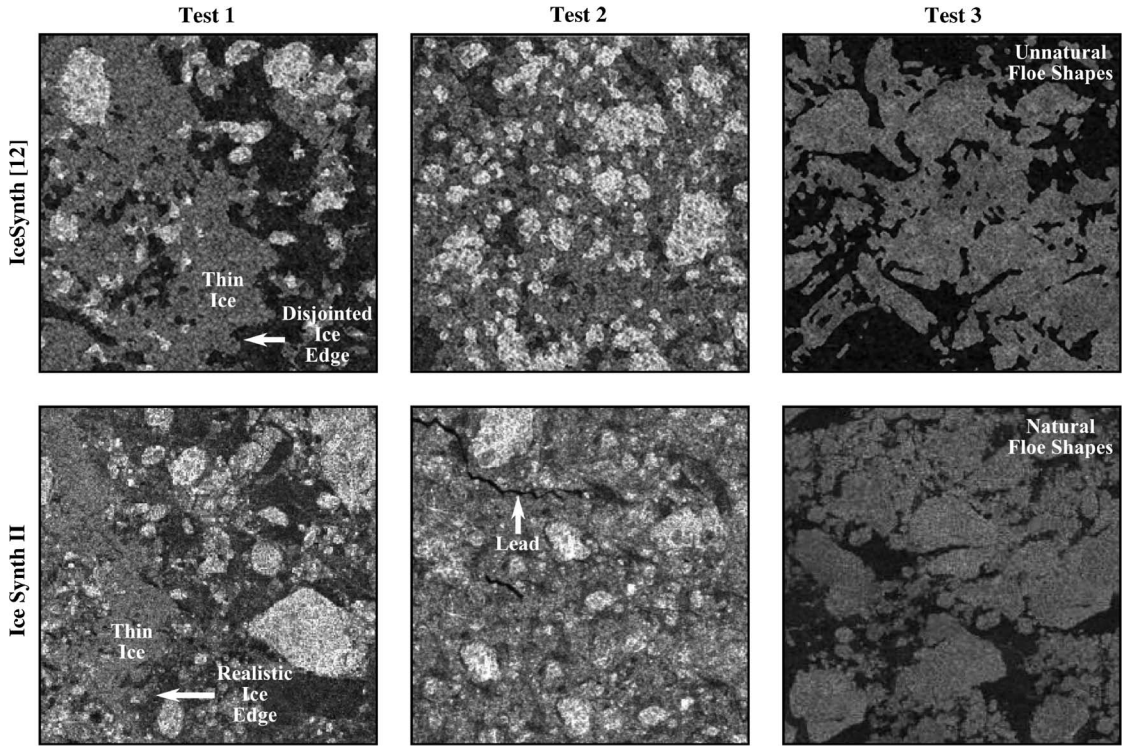

Fig. 2. Synthesized SAR sea-ice images produced using the tested methods for an operational RADARSAT-1 single-polarization (HH) SAR sea-ice image. The synthetic imagery produced using IceSynth II performs noticeably better than the IceSynth system at capturing the multiscale structural characteristics of real SAR sea-ice imagery while not exhibiting a disjoint appearance at the structural boundaries.

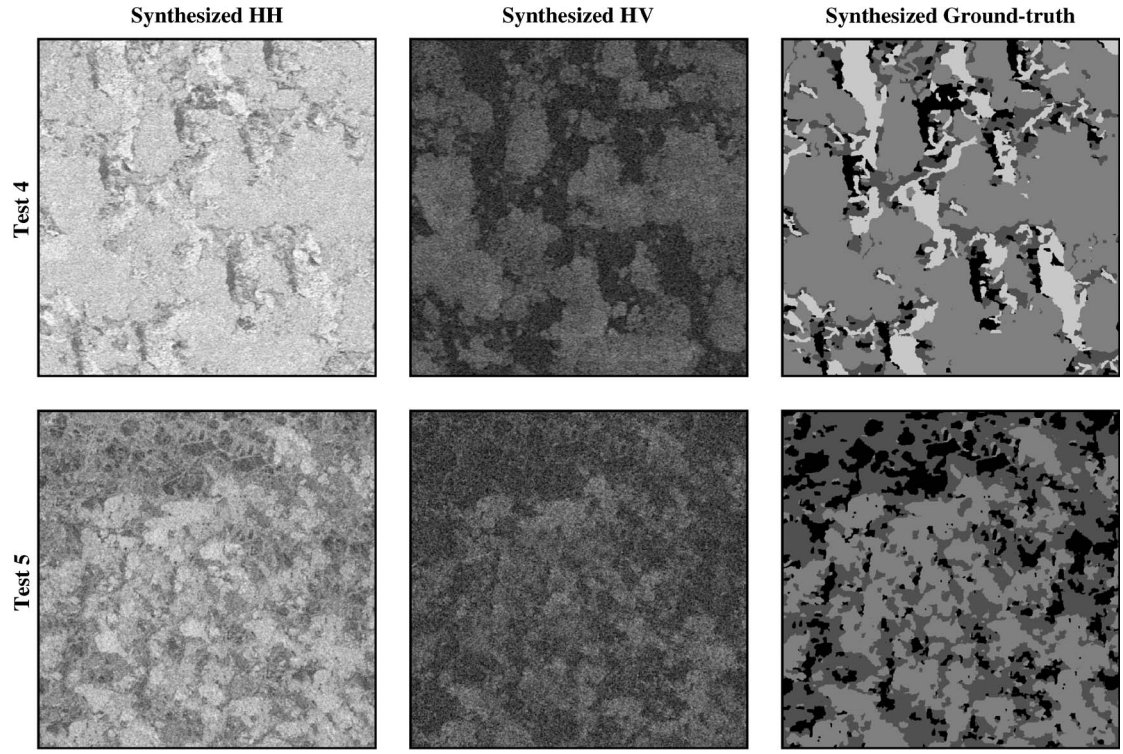

Fig. 3. Synthesized SAR sea-ice images and associated ground-truth segmentations produced using IceSynth II for operational RADARSAT-2 dual-polarization (HH and HV) SAR sea-ice imagery.

previous approaches, the proposed sampling approach allows synthetic SAR sea-ice imagery and the associated ground-truth segmentation to be generated for any arbitrary size, provided ground truth for the real image is available.

III. Experimental Results

To demonstrate the effectiveness of IceSynth II at producing natural looking and realistic SAR sea-ice imagery, synthetic images were generated based on three sea-ice test sets:

one operational RADARSAT-1 single-polarization (HH) image and two RADARSAT-2 dual-polarization (HH and HV) images provided by CIS. The objective is to use relevant CIS operational data to support automated classification such as MAGIC [15]. For comparison purposes, the IceSynth synthesis system proposed in [11] was also tested for the single-polarization image. The dual-polarization imagery was not tested with IceSynth [11] because it lacks multiband image support. Although IceSynth II can synthesize an arbitrary number of channels, quad-polarization source images were not available for testing. All tested images have 8-b pixel values that map the calibrated backscatter coefficient σ° in decibels to [0, 255].

The synthesized SAR sea-ice images produced using the tested methods for operational RADARSAT-1 single-polarization (HH) SAR sea-ice imagery are shown in Fig. 2. While both methods capture the nonhomogeneous textural characteristics of SAR sea-ice imagery, the synthetic imagery produced with IceSynth II appears more natural looking and without the disjoint appearance at the structural boundaries produced using IceSynth [11]. This is indicated by the ice edge shown for Test 1, which is a boundary between fairly thin, unconsolidated ice and water. IceSynth [11] produces a very well-defined edge which is unnatural since the ice is too new to hold together. In contrast, a similar result generated by IceSynth II reflects the natural tendency for thin ice to break up at the ice-water edge, resulting in a much less well defined edge. In Tests 2 and 3, IceSynth II performs noticeably better than the IceSynth system at capturing the multiscale structural characteristics of real SAR sea-ice imagery. Realistic leads are produced and the shape of the floes, being rounder and with less well defined edges, are much more natural. This demonstrates the effectiveness of IceSynth II in generating realistic-looking synthetic SAR sea-ice imagery that can be used for systematic and reliable comparison of automated SAR sea-ice segmentation algorithms.

The synthesized SAR sea-ice images produced using IceSynth II for RADARSAT-2 dual-polarization (HH and HV) SAR sea-ice imagery are shown in Fig. 3. As with previous cases, the synthesized HH and HV images appear natural looking and capture both the nonhomogeneous textural and multiscale structural characteristics of real SAR sea-ice imagery. The synthesized ground-truth images, generated from visual segmentations of the source images, are shown to illustrate that the algorithm can synthesize a ground-truth image if the source images have a pixel-level ground-truth segmentation. Given the potential of HV information in improving SAR sea-ice segmentation and classification, the ability to generate realistic looking dual-polarization SAR sea-ice imagery is very important in future sea-ice analysis techniques.

IV. Conclusion

This letter introduced IceSynth II, a novel method for generating synthetic SAR sea-ice imagery based on real SAR sea-ice priors. A region-based local conditional posterior sampling scheme was used to generate both the synthetic images and the associated ground-truth segmentations. Synthesis results demonstrate the effectiveness of IceSynth II for synthesizing more realistic-looking SAR sea-ice images than previous methods, making it well suited for use in systematic evaluation of SAR sea-ice image segmentation methods. Future work involves extending IceSynth II to allow for greater control over the generated imagery, such as allowing for user-defined sea-ice proportions and floe and lead sizes.

Acknowledgment

The source SAR images were provided by the CIS and are copyrighted by the Canadian Space Agency.

References

[1] D. Flett, M. Manore, B. Ramsay, and J. Falkingham, "Preparing for operational use of RADARSAT-2 data at the Canadian Ice Service," in *Proc. IEEE Int. Geosci. Remote Sens. Symp.*, 2001, vol. 1, pp. 493–495.

[2] R. Samadani, "A finite mixture algorithm for finding proportions in SAR images," *IEEE Trans. Image Process.*, vol. 4, no. 8, pp. 1182–1186, Aug. 1995.

[3] Q. Remund, D. Long, and M. Drinkwater, "Polar sea-ice classification using enhanced resolution NSCAT data," in *Proc. IEEE Int. Geosci. Remote Sens. Symp.*, 1998, vol. 4, pp. 1976–1978.

[4] J. Karvonen, "Baltic sea ice SAR segmentation and classification using modified pulse-coupled neural networks," *IEEE Trans. Geosci. Remote Sens.*, vol. 42, no. 7, pp. 1566–1574, Jul. 2004.

[5] L. Soh, C. Tsatsoulis, D. Gineris, and C. Bertoia, "ARKTOS: An intelligent system for SAR sea ice image classification," *IEEE Trans. Geosci. Remote Sens.*, vol. 42, no. 1, pp. 229–248, Jan. 2004.

[6] Q. Yu and D. A. Clausi, "SAR sea-ice image analysis based on iterative region growing using semantics," *IEEE Trans. Geosci. Remote Sens.*, vol. 45, no. 12, pp. 3919–3931, Dec. 2007.

[7] D. Blacknell, A. Blake, P. Lombardo, and C. Oliver, "A comparison of simulation techniques for correlated gamma and K-distributed images for SAR applications," in *Proc. IEEE IGARSS*, 1994, vol. 4, pp. 2182–2184.

[8] D. Blacknell, "A new method for the simulation of K-distribution clutter," *Proc. Inst. Elect. Eng.—Radar Sonar Navig.*, vol. 141, no. 1, pp. 53–58, Feb. 1994.

[9] H. Cantalloube, "Texture synthesis for SAR image simulation," *Proc. SPIE*, vol. 3497, pp. 242–250, 1998.

[10] Y. Wu, C. Wang, H. Zhang, X. Wen, and B. Zhang, "Statistical analysis and simulation of high-resolution SAR ground clutter data," in *Proc. IEEE Int. Geosci. Remote Sens. Symp.*, 2008, vol. 4, pp. 2182–2184.

[11] A. Wong, W. Zhang, D. A. Clausi, and P. Fieguth, "IceSynth: An image synthesis system for sea-ice segmentation evaluation," in *Proc. Can. Conf. CRV*, Kelowna, BC, Canada, May 25–27, 2009, pp. 178–183.

[12] C. Oliver and S. Quegan, *Understanding Synthetic Aperture Radar Images*. Norwood, MA: Artech House, 1998.

[13] M. Vandewal, R. Speck, and H. Süß, "Efficient SAR raw data generation including low squint angles and platform instabilities," *IEEE Geosci. Remote Sens. Lett.*, vol. 5, no. 1, pp. 26–30, Jan. 2008.

[14] S. Z. Li, *Markov Random Field Modeling in Image Analysis*. New York: Springer-Verlag, 2001.

[15] D. A. Clausi, A. K. Qin, M. S. Chowdhury, P. Yu, and P. Malliard, "MAGIC: MAp-guided ice classification system," *Can. J. Remote Sens.*, Apr. 2009, to be published.